




Investigation of magnesium hydroxide functionalized by polydopamine/transition metal ions on flame retardancy of epoxy resin

Danping Zhu¹ · Qingqing Bi^{2,3} · Guang-Zhong Yin^{4,6} · Yan Jiang¹ · Wanlu Fu⁵ · Na Wang^{1,5} · De-Yi Wang^{4,6} 

Received: 8 January 2022 / Accepted: 18 June 2022 / Published online: 14 August 2022
© Akadémiai Kiadó, Budapest, Hungary 2022

Abstract

Aiming to impart epoxy resin (EP) with flame retardancy, magnesium hydroxide (MDH) was sequentially functionalized with four transition metals and polydopamine (PDA) to prepare MDH@M-PDA (M includes Fe³⁺, Co²⁺, Cu²⁺, Ni²⁺). Compared with MDH, MDH@M-PDA presented better dispersion in EP matrix. The results illustrated that a 30 mass% of MDH@Fe-PDA imparted the EP matrix with best fire retardancy and thermal stability. Specifically, the resultant EP/MDH/MDH@Fe-PDA composites remarkably reduced flammability, which is reflected by high LOI value of 29.3% and UL-94 V-0 ratings. The peak heat release rate (PHRR) and total smoke production (TSP) were reduced by 52% and 21%, respectively. Moreover, the impact and tensile strength of EP/MDH/MDH@M-PDA composites are improved compared with EP/MDH due to the better chemical compatibility of PDA in the EP matrix. Notably, this work provided a feasible design for organo-modified MDH and enriched its practical applications of MDH as functional fillers to polymers.

Keywords Epoxy resin (EP) · Magnesium hydroxide (MDH) · Transition metals, Polydopamine (PDA) · Flame retardant

Danping Zhu, Qingqing Bi have been contributed equally to this work.

✉ Na Wang
iamwangna@syuct.edu.cn

✉ De-Yi Wang
deyi.wang@imdea.org

¹ Liaoning Provincial Key Laboratory for Preparation and Application of Special Functional Materials, Shenyang University of Chemical Technology, Shenyang 110142, China

² China-Spain Collaborative Research Center for Advanced Materials, College of Materials Science and Engineering, Chongqing Jiaotong University, Chongqing 400074, China

³ College of Civil Engineering, Chongqing Jiaotong University, Chongqing 400074, China

⁴ IMDEA Materials Institute, C/ Eric Kandel, 2, 28906 Getafe, Madrid, Spain

⁵ Shenyang Research Industrial Technology for Advanced Coating Materials, Shenyang 110142, China

⁶ Universidad Francisco de Vitoria, Ctra. Pozuelo-Majadahonda Km 1,800, 28223 Pozuelo de Alarcón, Madrid, Spain

Introduction

Epoxy resins (EP) have prominent mechanical property, agglutinate property, electrical insulating and thermal stability, etc., which is widely applied in aerospace, automotive and electronic devices [1–6]. However, EP has high flammability, which will imperil to life safety and environmental safety, and restricting the practical applications in a number of fields [7, 8]. Therefore, improvement of the flame retardancy of EP composites is essential and adding flame retardant into EP resins is an effective method to change its flammability disadvantages. In the existing flame retardant system, halogen flame retardant has good flame-retardant properties, while it is forbidden because of its threat to environment and human health [9–13]. Over the past time, as a halogen-free flame retardant, magnesium hydroxide (MDH) has received widespread attention in terms of polymer flame retardant with the advantages of non-toxicity, environmentally friendly, and good smoke-suppressing properties [14, 15]. However, compared with halogen flame retardants, to achieve a considerable flame retardant effect, the filling amounts should generally reach more than 60 mass% [16–18]. MDH as an inorganic material, if its filling amount reaches a high value in the EPs, their mechanical properties

will be reduced significantly. MDH often needs further modification to improve the impact properties, tensile strength and other mechanical properties of composite materials. For examples, Meng et al. [14] prepared bio-based flame retardant (MDH@M-Phyt, M = Cu, Zn) by precipitation method, which acted in the PVC matrix. Compared with PVC/MDH, 10 phr PVC/MDH@M-Phyt had increased flame retardant and mechanical properties, and the peak heat release rate of MDH@Zn-Phyt had decreased by 33.5%. Yao et al. [16] synthesized boric acid (BA) crosslinked polyphosphazene (PZN)-modified MDH (MDH-PZPI-BA) and used ethylene vinyl acetate (EVA) as matrix. The tensile strength and elongation at break of 55 mass% EVA/MDH-PZPI-BA were enhanced by 26.1% and 33.5% compared to EVA/MDH. Therefore, it was promising and worthwhile to improve the mechanical properties of modified MDH composites, accompanied by the maintenance of MDH fire retardancy.

In recent years, dopamine hydrochloride (DOPA) had attracted wide attention because of its various surface deposition properties [19–21]. In an alkaline aqueous solution, DOPA can form polydopamine (PDA) through self-polymerization [20]. Because PDA has strong adhesion on various surfaces, it can be used as a universal surface modifier, which has applications in electrochemistry, biomedical engineering, membrane technology, etc. [21–24]. In addition, PDA can simultaneously provide a large number of active catechol groups for further modification and free radical scavenging ability, which strongly indicates that PDA can be used to modify the surface of MDH flame retardants [25, 26]. In addition, it has been found that transition metal compounds can improve the flame-retardant and smoke-suppressing properties of composites [27]. For example, the chelation reaction of iron ion, copper ion, cobalt ion and nickel ion with the ligand with flame retardant element can improve the flame retardant performance of the flame retardant ligand [28–34].

In the study, one-pot reaction was used to prepare flame-retardant composite materials, polydopamine (PDA) was loaded with transition metal ions to modify magnesium hydroxide, and unmodified magnesium hydroxide was used as a control group for comparative experimental study. In study, the mechanical, flame retardant, and smoke-suppressing properties of epoxy resin compounds were studied.

Experimental

Materials

MDH was bought from Liaoning Jinghua New Material Co., Ltd (Liaoning, China). Tris (hydroxymethyl) aminomethane (Tris), iron (III) chloride (FeCl_3), Cobalt (II) chloride (CoCl_2), Nickel (II) chloride (NiCl_2) and Copper

(II) chloride (CuCl_2) were obtained from Tianjin Damao Chemical Reagent Factory (Tianjin, China). 4,4-Dimino-diphenyl sulfon (DDS) and Dopamine hydrochloride (DOPA) were purchased from Shanghai Macklin Biochemical Co., Ltd (Shanghai, China). EP (EP-44) was supplied by Nantong Xingchen Synthetic Material Co., Ltd (Nantong, China). All reagents were of analytical grade purity and were used as received.

Synthesis of MDH@M-PDA composites

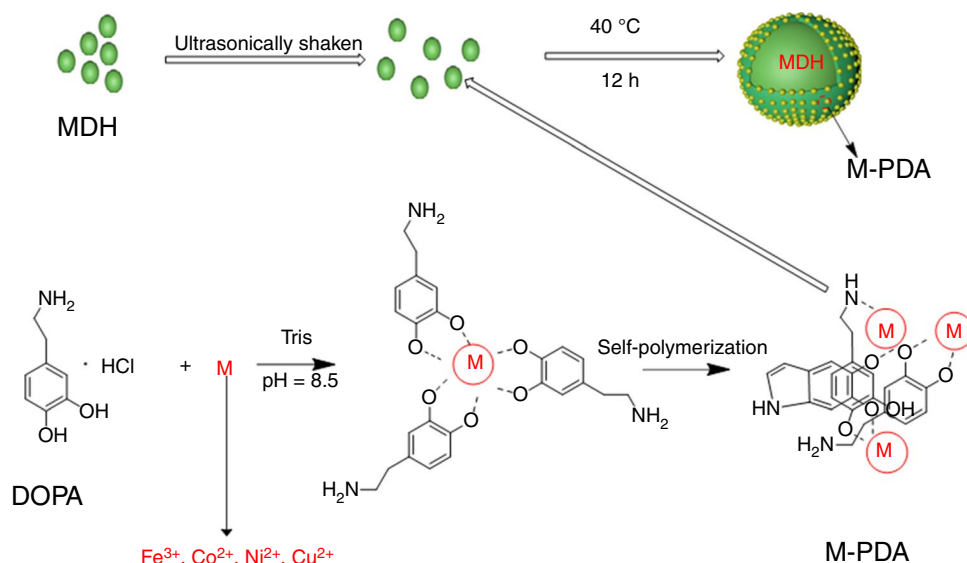
MDH (5 g) was added to there-necked equipped with deionized water (1000 mL) and ultrasonically shaken for 30 min. After that, dopamine hydrochloride (DOPA, 5 g) and Cobalt chloride (CoCl_2 , 0.6 g) were added to MDH solution under conditions. The pH was adjusted to 8.5 with Tris buffer and stirred at 40 °C for 12 h [35]. Subsequently, the solution was washed with deionized water. Subsequently, it was soaked in deionized water and slowly stirred for three days to remove unbound PDA. Finally, the product as MDH@Co-PDA was collected after filtering, washing with deionized water, drying at 60 °C. MDH@Fe-PDA, MDH@Ni-PDA, and MDH@Cu-PDA were prepared by the same method. The route for synthesis is illustrated in Scheme 1.

Preparation of EP and EP composites

A 100 mL beaker containing EP (10 g) and DDS (3.57 g) was placed in an oil bath at 150 °C and with vigorous magnetic stirring. After the curing agent was completely dissolved into a brownish yellow solution, MDH and MDH@M-PDA were added to the solution and stirred for 3 min. After that, the mixture was put to a vacuum oven to degas for 2 min and then poured it into the iron mold which was needed to be preheated in the 160 °C oven and coated with dimethylsilicone oil as release agent. The curing procedures were set at 160 °C for 1 h, 180 °C for 2 h and 200 °C for 1 h, and the heating rate was 2 °C min^{-1} [3]. The above method was used to prepare other products, and the detailed ratio is shown in Table 1.

Characterizations

The elements in flame retardants were analyzed energy-dispersive X-ray spectroscopy (EDX). The scanning electron microscope (SEM) obtained by JEOL JSM-6360LV showed the microscopic morphology of the flame-retardant. X-ray diffraction (XRD) characterized the crystalline form of diffraction patterns and XRD was acquired by D8-ADVANCE with a target of Cu-K α . The molecular structure of the flame-retardant was characterized by Fourier transform infrared (FTIR) spectra, which was collected on Nicolet MNGNA-IR560 infrared spectrometer

Scheme 1 Synthesis route of MDH@M-PDA composites**Table 1** Composition of the samples

Sample	Epoxy resin/g	4,4-Dimethylnodiphenyl sulfon/g	MDH/g	MDH@M-PDA/g
EP	10	3.57	–	–
EP/MDH	10	3.57	3	–
EP/MDH/MDH@M-PDA	10	3.57	2.3	0.7

M includes Fe^{3+} , Co^{2+} , Cu^{2+} , Ni^{2+}

in the range from 4000 to 400 cm^{-1} at room temperature. Limiting oxygen index (LOI) and vertical combustion (UL-94) generally analyzed the flame retardant of composite materials. UL-94 measurements were carried out by ASTM D380, and the sheet size was $127 \times 12.7 \times 3 \text{ mm}^3$. LOI values were conducted on JF-3 oxygen index instrument, and it provided a sheet dimension was $127 \times 6.5 \times 3 \text{ mm}^3$ by ASTM D2863-13. The thermal decomposition process of composites was presented by thermogravimetric analysis (TGA), which is heated to 800 $^{\circ}\text{C}$ by STA449C under nitrogen at a rate of 10 $^{\circ}\text{C min}^{-1}$. The combustion performance of the composite material was presented by the cone calorimetry test, which was based on ISO 5660-1 with a heat flux of 50 kW m^{-2} and the sample size was $100 \times 100 \times 4 \text{ mm}^3$. The composition of residual char was studied by Raman spectroscopy, which was obtained by Horiba science LabRAM HR at 523 nm laser. Impact test of unnotched splines was conducted on an impact testing machine, according to ISO 2932003. Tensile test was performed on the tensile testing machine (9250 HV, Instron Engineering Corporation) following GB/T528-2009 procedure.

Results and discussion

Structure of MDH@M-PDA flame retardants

The morphology of MDH and MDH@M-PDA were observed by SEM. Figure 1a shows the block structure of MDH, which indicates that MDH was agglomerated obviously. Figure 1b–e shows the surface of MDH after modification that the level of disaggregation of particles is improved, which may improve the dispersion of MDH-related particles in the polymer matrix. Then, EDX tests are carried out for MDH@Co-PDA, MDH@Cu-PDA, MDH@Ni-PDA and MDH@Fe-PDA as shown in Fig. 2a–b. The contents of different transition metal ions of MDH@M-PDA are listed in Table 2. The result shows that the modified MDH has transition metal elements and Mg elements, surrounding on the particle surface [36].

The Fourier transform infrared spectra of the FRs are shown in Fig. 3. For PDA, the typical peaks that emerged at 3347 cm^{-1} and 1498 cm^{-1} are attributed to the stretching vibration of carbonyl group in catechol structure and shear vibration of N–H bonds [21]. For MDH, the typical peak at 3702 cm^{-1} corresponds to -OH. There are some differences about some special peaks of MDH@Fe-PDA. For example, the typical peaks of PDA at 3347 cm^{-1} and 1498 cm^{-1} almost disappear in MDH@Fe-PDA peaks, which is attributed to tendency of Fe^{3+} to combine with the O atoms of the carbonyl group and the N atoms of the amino group [35]. The MDH@Fe-PDA peak intensity (3702 cm^{-1}) was significantly reduced relative to that of MDH. It is probably due to that MDH surface was coated with PDA molecules with strong adhesion ability. Figure 3b shows FTIR spectra of MDH surface modification by PDA loaded with four transition metal ions. Figure 3a shows that the typical peaks

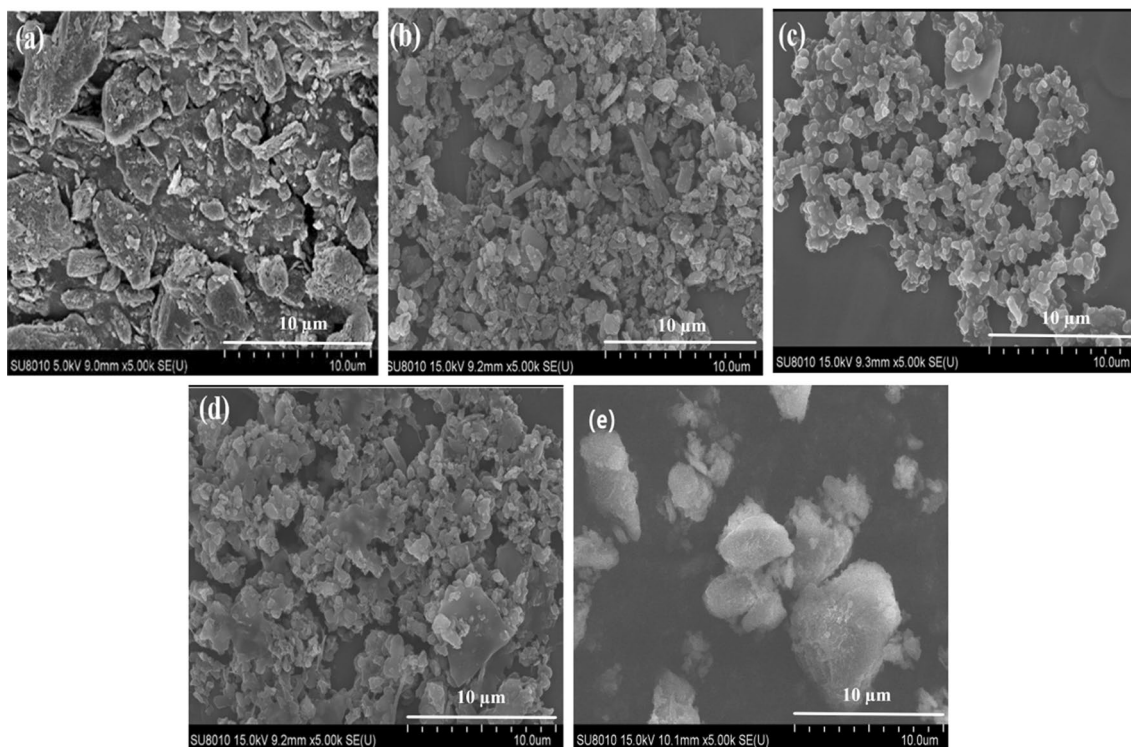


Fig. 1 SEM images of (a) MDH, b MDH@Co-PDA, c MDH@Cu-PDA, d MDH@Ni-PDA, e MDH@Fe-PDA

of MDH@Co-PDA, MDH@Ni-PDA, MDH@Cu-PDA and MDH@Fe-PDA are the same. It can be considered that Co^{2+} , Ni^{2+} and Cu^{2+} can also be combined with the C=O oxygen atom and NH nitrogen atom in PDA [37].

The XRD curves of MDH and MDH@M-PDA are shown in Fig. 4. Specifically, MDH@M-PDA also has the same typical XRD spectrum as MDH. This shows that the synthesis of modifier does not influence the crystal structure of MDH remarkably. Moreover, the several peaks located at 12.14° , 18.85° , 38.02° , 50.89° , 58.71° and 62.24° are ascribed to (001), (101), (102), (110), (111), (103) crystal faces of MDH, respectively.

Thermal stability of EP and EP composites

Thermal decomposition behavior and char residue of composite materials were carried out by TGA in the atmosphere of N_2 . The relating experimental parameters are listed in Table 3, and the curves are shown in Fig. 5. After adding Fe-PDA, the $T_{5\%}$ ($T_{5\%}$ is defined as the temperature corresponding to 5 mass% mass loss) of EP/MDH composites decreased by 2°C . This is mainly because Fe-PDA has the ability to catalyze carbonization, which will cause composite to decompose in advance [3]. Although the addition of flame

retardant did not increase the $T_{50\%}$ of the composites, the C_{750} (C_{750} means char yield at 750°C) of the composites increased. EP/MDH had the highest C_{750} at 30%, mainly because MDH decomposes endothermically and forms stable oxides on the surface of the composite. Moreover, after adding MDH@M-PDA, the C_{750} of the composites is no different from that of EP/MDH (Fig. 6).

Combustion behavior

The flammability of composites is investigated by limiting oxygen index (LOI) and vertical combustion burning tests (UL-94). The LOI value is 20.5% for pure epoxy resin and its UL-94 vertical burning test exhibited no rating. The LOI value of composites with 30 mass% MDH increases significantly to 26.5%. It is because MDH itself has the potential of endothermic decomposition, and it can reduce the surface temperature of the sample. During the ignition process, a protective oxide layer with highly quality and not easily decomposed by heat is formed on the polymer surface to further prevent polymer degradation, and it improves the flame-retardant of composites [14]. MDH is modified by Fe-PDA, Co-PDA, Cu-PDA and Ni-PDA, respectively, and adds to EP/MDH composites to improve the LOI value of EP

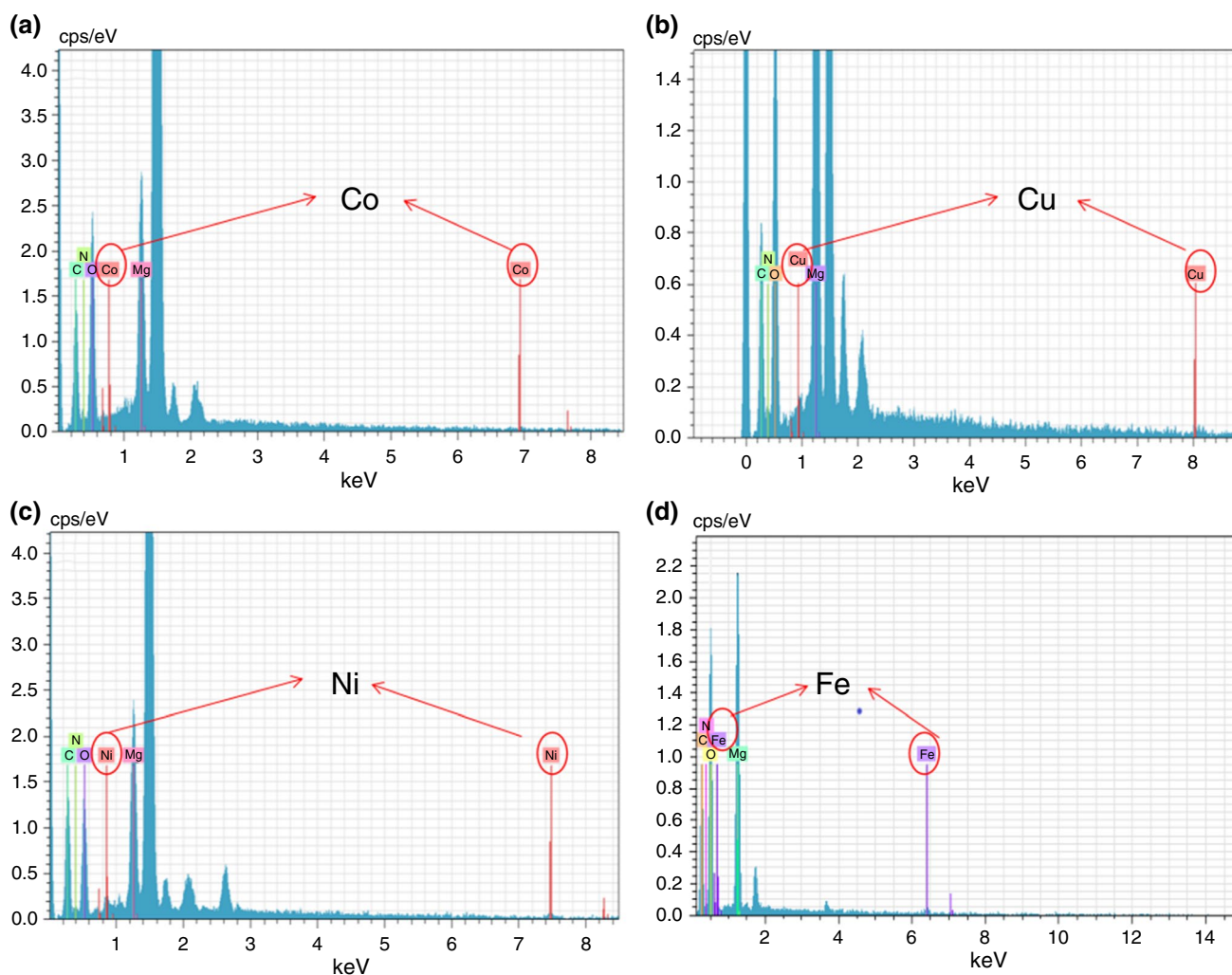


Fig. 2 EDX data of (a) MDH@Co-PDA, b MDH@Cu-PDA, c MDH@Ni-PDA, d MDH@Fe-PDA

Table 2 The content of atoms

Sample	SEM (The content of atoms/mass%)				
	O	C	Mg	N	M
MDH@Co-PDA	46.07	29.50	16.09	7.97	0.37
MDH@Cu-PDA	38.18	25.12	31.22	3.69	1.78
MDH@Fe-PDA	45.52	30.70	17.63	3.78	2.36
MDH@Ni-PDA	35.42	37.43	15.64	7.06	4.45

M includes Fe^{3+} , Co^{2+} , Cu^{2+} , Ni^{2+}

composites, which shows that different kinds of transition metal ions can promote the flame-retardant of composites in varying degrees. Notably, the composites containing Fe^{3+} with the highest LOI value (29.3%) and passes UL-94 V-0 rating. This is mainly because the catalytic performance of

Fe^{3+} is higher than that of the other three transition metals, so that more graphitic carbon is generated when the composite is burned, thereby improving the quality of carbon residue. This is consistent with Raman spectra results.

For a more detailed simulation of a realistic fire scenario, cone calorimeter test (CCT) is carried out for EP and EP composites [38, 39]. EP exhibits a peak heat release rate (pHRR) of $718 \pm 18 \text{ kW m}^{-2}$ at 114 s (Fig. 7a). Compared with pure EP, EP composites with 30 mass% pristine MDH have a slower heat release rate (HRR). Moreover, compared with EP materials and EP/MDH, MDH@M-PDA-modified EP/MDH composite materials have lower exothermic strength and slower HRR. Typically, the EP/MDH/MDH@Cu-PDA performs the lowest pHRR. This indicates that Cu^{2+} can effectively protect the EP matrix from heat and combustible gases. EP/MDH/MDH@Cu-PDA increases the

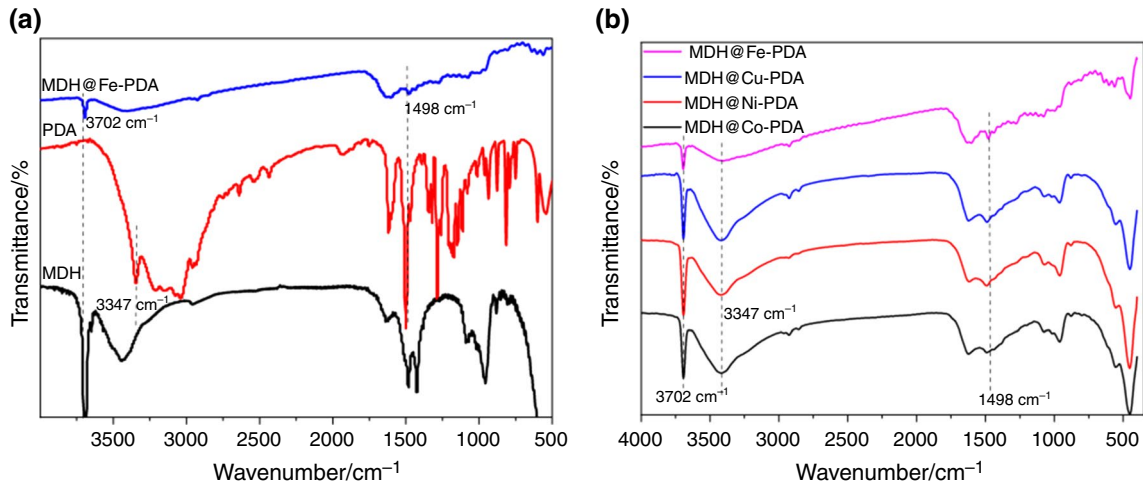


Fig. 3 a FTIR spectra of MDH@Fe-PDA, PDA and MDH, b FTIR spectra of MDH@M-PDA

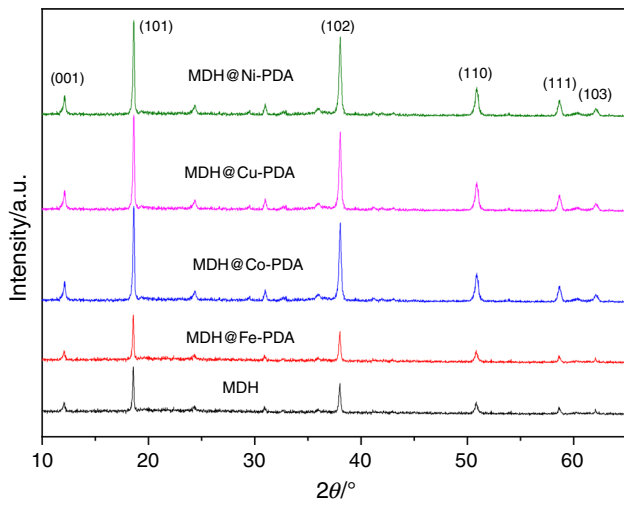


Fig. 4 XRD patterns of MDH, MDH@Fe-PDA, MDH@Cu-PDA, MDH@Co-PDA and MDH@Ni-PDA

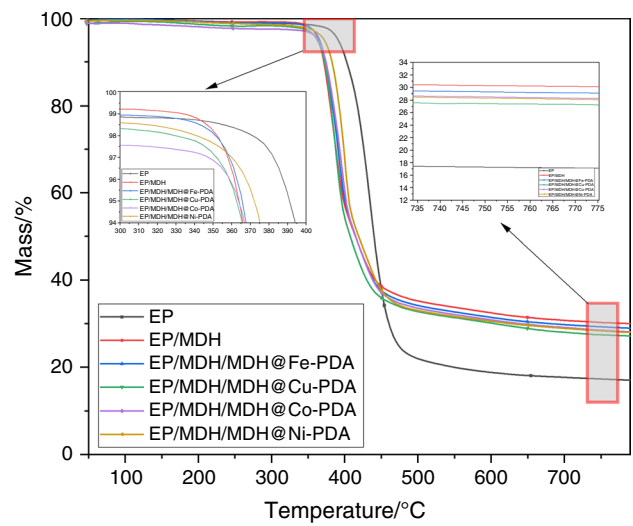


Fig. 5 TGA curves of composite materials

Table 3 The TGA data of composites

Sample	T _{5 mass%} /°C	T _{50 mass%} /°C	Residue at 750 °C/% (C ₇₅₀)
EP	390	439	17
EP/MDH	363	413	30
EP/MDH/MDH@Fe-PDA	365	413	29
EP/MDH/MDH@Co-PDA	361	410	27
EP/MDH/MDH@Cu-PDA	362	414	28
EP/MDH/MDH@Ni-PDA	372	418	28

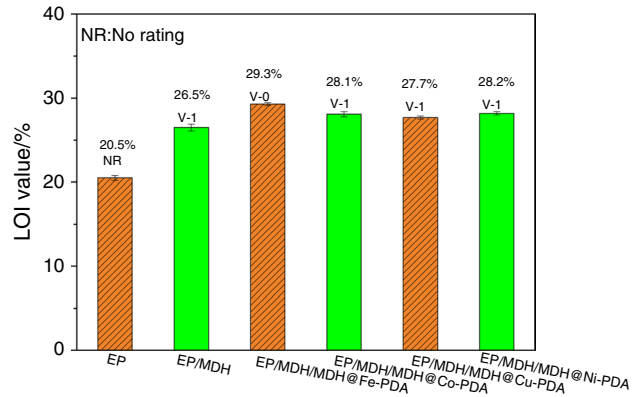


Fig. 6 Flame retardancy of the samples

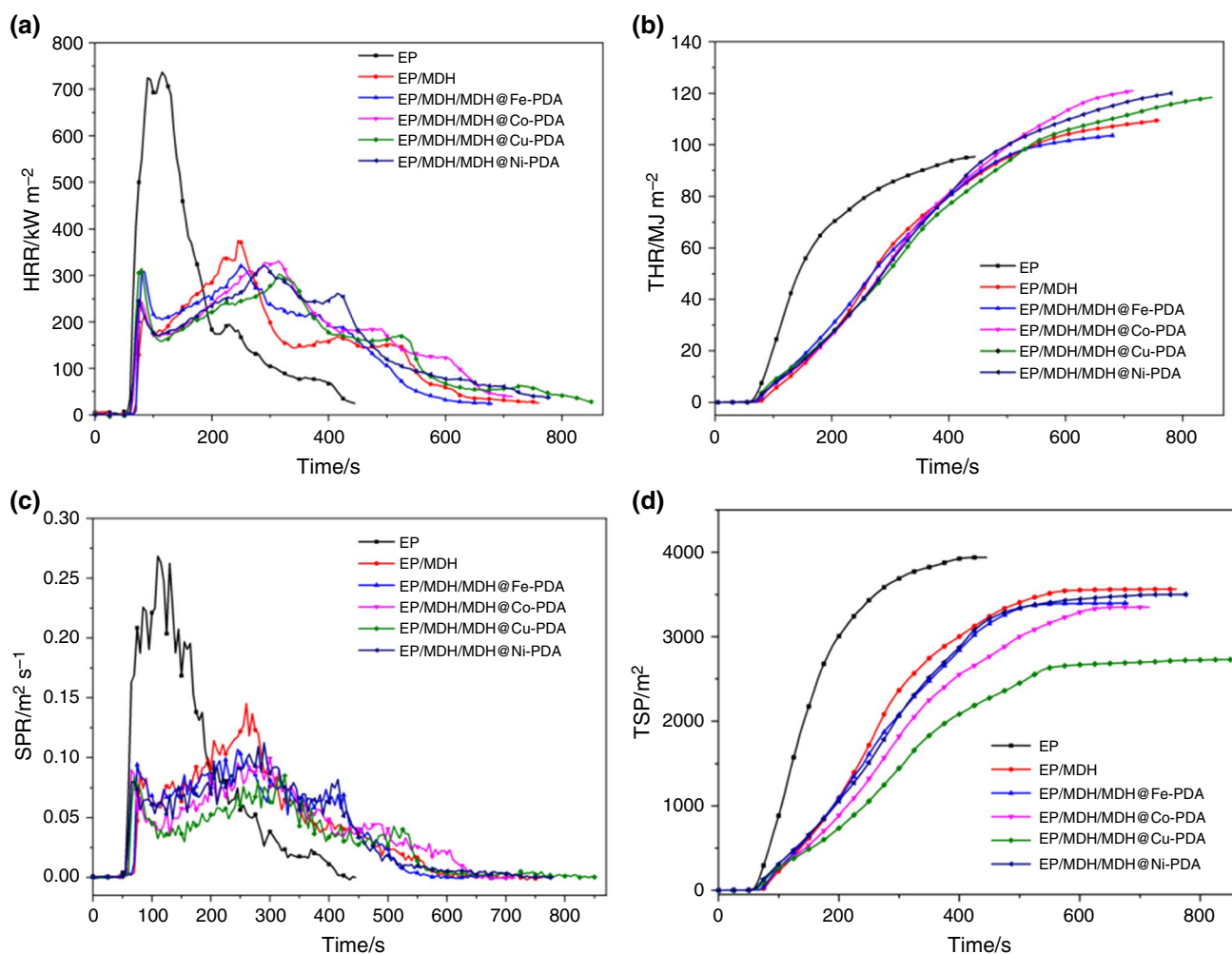


Fig. 7 **a** The heat release rate, **b** the total heat release, **c** the smoke production rate and **d** the smoke production curves of composites

burning time from 445 to 850 s compared with EP (Fig. 7b). It indicates that the combustion behavior changes from typical non-carbonized material (EP) to typical carbonized material (EP/MDH/MDH@Cu-PDA) to further extend the burning time.

In a fire hazard, the main cause of the critical factor concerning human survival is a large amount of toxic smoke and toxic gas produced by polymer matrix in the fire [32]. Thus, improving the smoke suppression of polymer materials has important practical significance [40–42]. It can be seen in Fig. 7c, the curves of the smoke production rate (SPR), and it has a similar trend to that of the heat release rate (HRR), which is probably due to the burning of more volatiles, thereby producing more heat release and combustion product. The peak of SPR (pSPR) values of the EP composites with addition of MDH has reduced to $0.144 \text{ m}^2 \text{ s}^{-1}$. It is due to that the endothermic decomposition of MDH and the release of nonvolatile gas delay the combustion rate,

and the metal oxide is produced by MDH forms a protective layer on the surface of EP composites, which will block the transmission of combustible gas and heat radiation, so as to inhibit the combustion of decomposed gas [43]. Moreover, the pSPR of EP/MDH/MDH@M-PDA (M here refers to Fe^{3+} , Co^{2+} , Cu^{2+} , and Ni^{2+} in turn) is reduced to $0.106 \text{ m}^2 \text{ s}^{-1}$, $0.100 \text{ m}^2 \text{ s}^{-1}$, $0.085 \text{ m}^2 \text{ s}^{-1}$, $0.112 \text{ m}^2 \text{ s}^{-1}$. The possible reason is that the catechol functional group in PDA has strong free radicals scavenging activity, which can remove the generated free radicals during combustion to inhibit the combustion and degradation rate of EP composites and to correspondingly reduce the supply of gaseous fuel, toxic gases and the emission of smoke [44]. In addition, transition metal ions have the ability to catalyze carbonization and can catalyze the composites to form more aromatic char during the combustion process [45]. Cu^{2+} can effectively control the smoke release rate (SRR) in the combustion process of EP composites. So that, SRR and TSP of EP/MDH/MDH@

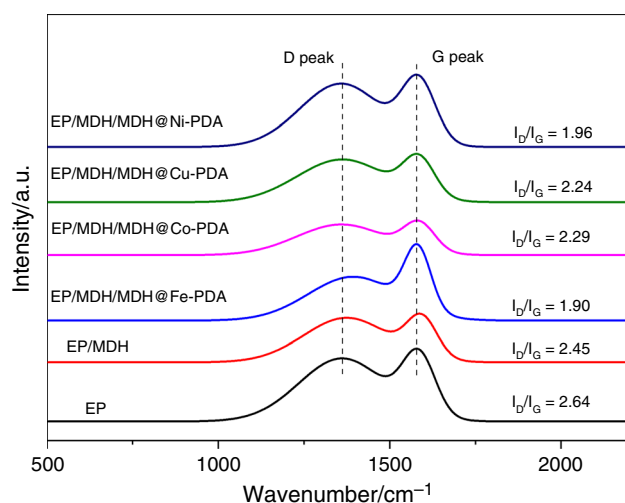


Fig. 8 Raman spectra of CCT chars

Table 4 The impact strength, tensile strength and elongation at break data of EP and EP composites

Sample	Impact strength/kJ m ⁻²	Tensile strength/Mpa	Elongation at break/%
EP	4.674	27.72	5.83
EP/MDH	5.881	37.91	10.22
EP/MDH/MDH@Fe-PDA	9.129	43.29	11.77
EP/MDH/MDH@Co-PDA	7.377	43.51	10.56
EP/MDH/MDH@Cu-PDA	6.503	42.38	9.78
EP/MDH/MDH@Ni-PDA	9.167	40.06	10.56

Cu-PDA composites are always lower than other EP composites, which has excellent flue gas control effect.

In order to clarify the flame retardant mechanism of EP composites, the residual char composition of composites is investigated using the Raman spectra (Fig. 8). It is worth noting that the peaks at 1338 cm⁻¹ and 1600 cm⁻¹ are owned to the A_{1g} ring stretching vibration mode of disordered carbon (D peak), first-order scattering of the E_{2g} symmetric vibration mode of graphite carbon (G peak) [20]. In addition, the ratio of D peaks area (I_D) to G peaks area (I_G) reflects graphitization degree in the graphite planes in carbonized polymers [20, 46]. Here, MDH is added to EP, and the value of I_D/I_G is reduced to 2.45, and I_D/I_G of EP/MDH composites adding MDH@M-PDA is lower than that of EP/MDH, which releases more graphite carbon formed in modified EP/MDH composites residual char [47, 48]. This shows that transition metal ions play a certain catalytic role

in the carbonization of EP matrix, and the quality of residual char is improved, and it is same of the TGA and CCT results.

Mechanical behavior of EP composites

Non-notched impact tests and tensile tests were used to study the mechanical behavior of composites. Table 4 shows the impact strength, tensile strength and elongation at break data of EP and EP composites. It can be seen from Fig. 9a that the impact strength of neat EP is 4.674 kJ m⁻², and the impact strength of EP composites increases after adding flame retardant. Moreover, the impact strength of EP composites with MDH@M-PDA is higher than that of EP/MDH composites. It is possible that the surface energy of MDH functionalized by PDA is reduced and the surface polarity is changed, so that MDH can be better dispersed in EP matrix. In addition, the PDA has the hydroxyl and amine groups, and it has better chemical compatibility with EP [19]. Compared with EP/MDH, the addition of modified MDH significantly improves the impact strength. Typically, the impact strength of EP/MDH/MDH@Fe-PDA and EP/MDH/MDH@Ni-PDA is 9.1 kJ m⁻² and 9.2 kJ m⁻², respectively, an increase of 54.2% and 55.9%.

As shown in Fig. 9b, the stress–strain curves of EP composites belong to a typical brittle fracture characteristic. It can be seen from Fig. 9c that the tensile strength of EP (27.72 MPa) is the lowest. In detail, the tensile strength for EP/MDH/MDH@M-PDA exhibits an increase around 14.2%, 14.8%, 11.9% and 5.7% compared with EP/MDH composites (37.9 MPa). This is because after the compound is added to the surface functionalized MDH, the specific surface area of the compound increases and its surface polarity is reduced, thereby increasing the force between the matrix and the flame retardant, which increases the tensile strength. The agglomerates flame retardants become broken, which reduces the number of agglomerates of flame retardants in EP composites, thereby improving the tensile strength of EP composites. Moreover, as shown in Fig. 9d, EP/MDH/MDH@Fe-PDA has the highest elongation at break in all samples, and it may be caused by the better adhesion of the flame retardant with the effect of Fe³⁺ to the substrate, which makes EP composites to have better toughness. In order to study the dispersion of flame retardants in the matrix, SEM analysis of the cross section of EP composites was carried out. As shown in Fig. 10a–e, the cross section of the modified filler-filled composite material is more homogeneous, and there is no defect marked by the red circle in Fig. 10a, which indicated that the dispersion of fillers in the matrix

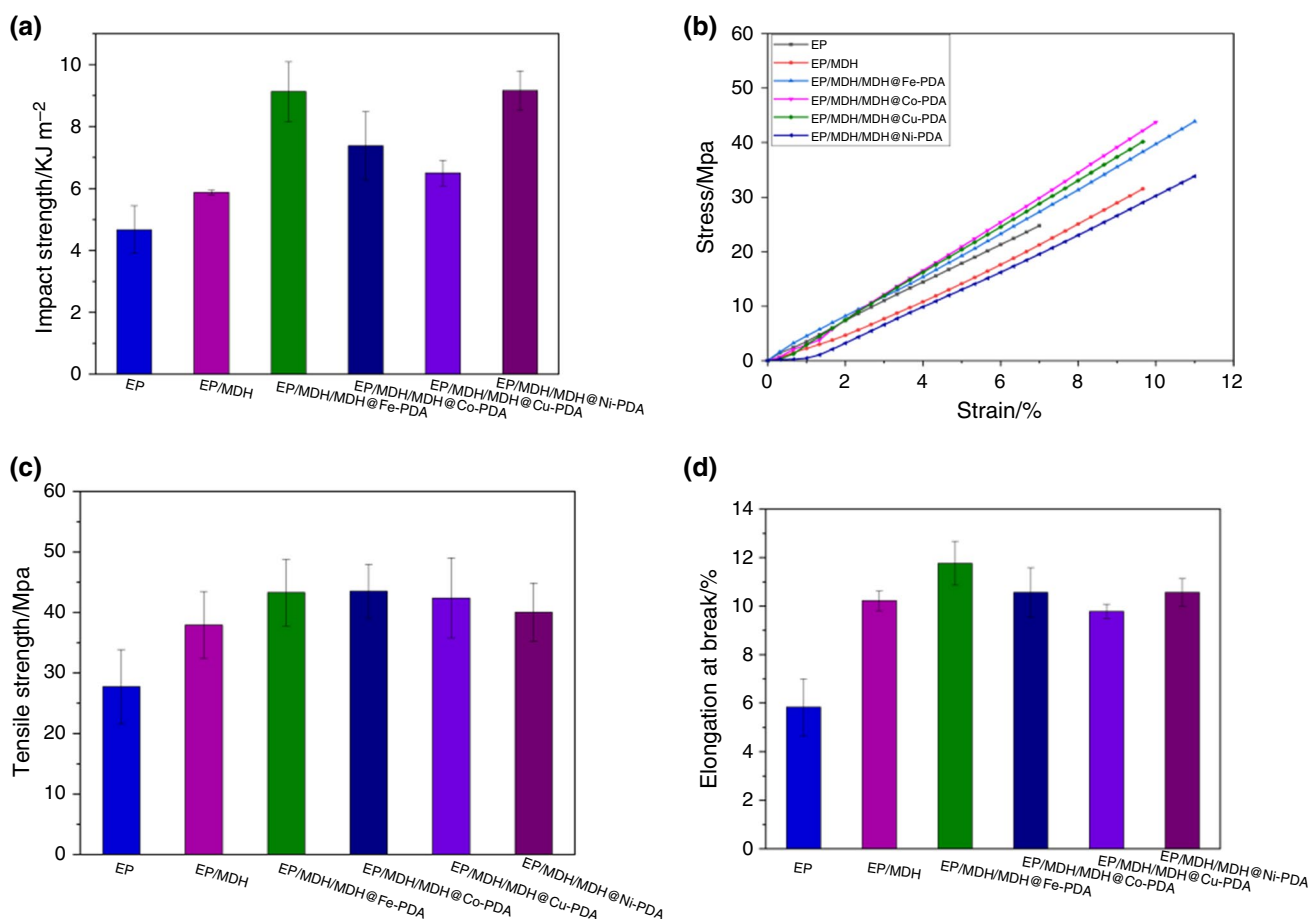


Fig. 9 **a** Impact strength of EP and EP composites, **b** Stress–strain curve of EP and EP composites, **c** Tensile strength of EP and EP composites, **d** Elongation at break of EP and EP composites

was improved to a certain extent. Figure 10f–i is the mapping diagram of M (M includes Fe, Co, Cu, Ni).

Flame-retardant mechanism of composites

Scheme 2 shows the flame retardant mechanism diagram of composite materials. Compared with EP/MDH composites, the EP/MDH/MDH@M-PDA composites have increased flame-retardant, smoke suppression and thermal stability, which mainly because M-PDA has the ability to catalyze carbonization and scavenge highly reactive radicals. In detail, for the EP/MDH/MDH@M-PDA composites, M-PDA can scavenge highly reactive radicals ($H\cdot$ and $OH\cdot$) which is produced during combustion of EP composites, which can reduce the fuel that is required for polymer combustion, and it can

improve the smoke suppression performance of polymer (see the CCT results). Meanwhile, transition metal ions can catalyze carbonization. M will promote the formation of char barrier with high degree of graphitization during EP composites. High quality residual char covers the surface of EP composites, so as to increase the thermal stability and flame-retardant of composites (see TGA, Raman spectroscopy results, Limit oxygen index and vertical combustion test). Moreover, the LOI value and UL-94 level of composites with flame retardant have greatly improved compared with EP, in which MDH plays a great role. MDH would produce nonflammable gas (H_2O) that diluted the concentration of oxygen and MgO , and MgO covers the polymer surface.

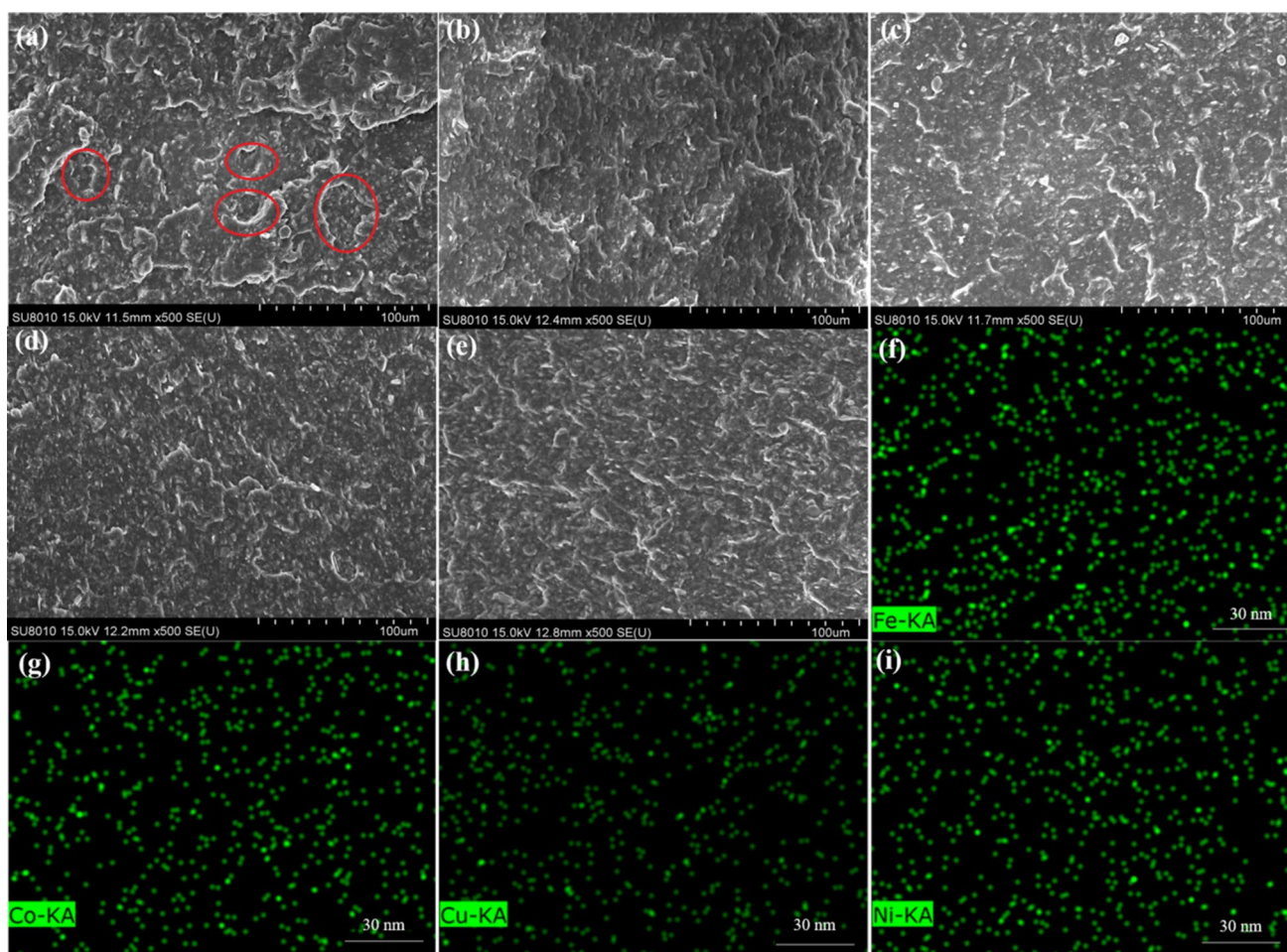
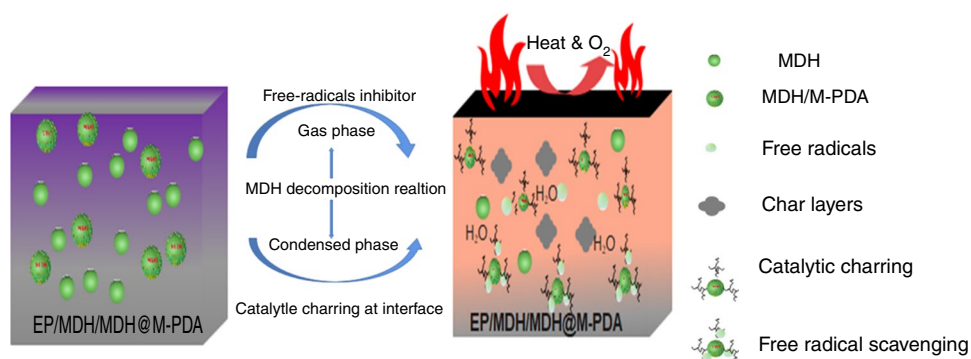


Fig. 10 SEM of the fractured surface morphology of (a) EP/MDH, b EP/MDH@Fe-PDA, c EP/MDH@Co-PDA, d EP/MDH@Cu-PDA, e EP/MDH@Ni-PDA, f Fe mapping of EP/MDH@Fe-PDA, g Co map-

ping of EP/MDH@Co-PDA, h Cu mapping of EP/MDH@Cu-PDA, i Ni mapping of EP/MDH@Ni-PDA

Scheme 2 Proposed flame retardant mechanism of composites



Conclusions

In this study, transition metal-loaded PDA-modified MDH was used as an additive flame retardant in EP composites. The smoke suppression, flame retardancy, and mechanical properties of composite materials were studied. The

results showed that adding modifier MDH@M-PDA can increase the flame-retardant and mechanical properties of EP/MDH. Those enhancements suppress smoke and flame-retardant were attributed to the ability of catalytic carbonization and intense radical scavenging activity of M-PDA. CCT result demonstrated that EP/MDH/MDH@

Cu-PDA had the best smoke suppression performance, and the optimal composite EP/MDH/MDH@Fe-PDA showed a limiting oxygen index of 29.3% and UL-94 reaching V-0 level compared with EP/MDH. In addition, the mechanical properties were improved, which was reflected in the increase in tensile and impact strength by 14.2% and 54.2%, respectively. Notably, through the comparison of mechanical properties, thermal stability, flame-retardant, and smoke-suppressing of flame retardants were modified by different transition metals, and it could be predicted which transition metals would be selected to modify the flame retardants in different fields.

Acknowledgements This work was financially supported by the National Natural Science Foundation of China, grant number 51973124; Technology for Producing Advanced Functional Mg-Based Chemicals, grant number 2020YFC1909302; Liao Ning Revitalization Talents Program, grant number XLYC2005002; “Jie Bang Gua Shuai” of Science and Technology Projects of Liaoning Province in 2021, grant number 2021JH1/10400091; Shenyang Science and Technology Program - Major Key Core Technology Project, grant number 20-202-1-15.

Authors' contributions DZ contributed to investigation, methodology, testing, and writing—original. QB contributed to investigation, methodology, testing, and writing—original. G-ZY contributed to methodology, testing, and writing—revision. YJ contributed to investigation, testing, and laboratory-support. WF contributed to testing. NW contributed to supervision, funding Support, and management. D-YW contributed to supervision, methodology, and writing—revision.

Declarations

Conflict of interest All authors have declare that they have no conflict of interest.

References

- Xu Y, Li J, Shen R, et al. Experimental study on the synergistic flame retardant effect of bio-based magnesium phytate and rice husk ash on epoxy resins. *J Therm Anal Calorim*. 2021. <https://doi.org/10.1007/s10973-020-10420-8>.
- Zhu ZM, Wang LX, Lin XB, et al. Synthesis of a novel phosphorus-nitrogen flame retardant and its application in epoxy resin. *Polym Degrad Stab*. 2019;169:108981. <https://doi.org/10.1016/j.polyimdegradstab.2019.108981>.
- Bi Q, Yao D, Yin GZ, et al. Surface engineering of magnesium hydroxide via bioinspired iron-loaded polydopamine as green and efficient strategy to epoxy composites with improved flame retardancy and reduced smoke release. *React Funct Polym*. 2020;155:104690. <https://doi.org/10.1016/j.reactfunctpolym.2020.104690>.
- Liang DX, Zhu XJ, Dai P, et al. Preparation of a novel lignin-based flame retardant for epoxy resin. *Mater Chem Phys*. 2021;259(17):124101. <https://doi.org/10.1016/j.matchemphys.2021.124101>.
- Huo SQ, Zhou ZX, Jiang JW, et al. Flame-retardant, transparent, mechanically-strong and tough epoxy resin enabled by high-efficiency multifunctional boron-based polyphosphonamide. *Chem Eng J*. 2022;427:131578. <https://doi.org/10.1016/j.cej.2021.131578>.
- Huo SQ, Song PG, Yu B, et al. Phosphorus-containing flame retardant epoxy thermosets: recent advances and future perspectives. *Prog Polym Sci*. 2021;114:101366. <https://doi.org/10.1016/j.progpolymsci.2021.101366>.
- Zhang Y, Yang W. Synthesis and characterization of PEDMCD as a flame retardant and its application in epoxy resins. *RSC Adv*. 2021;11(5):2756–66. <https://doi.org/10.1039/D0RA10233D>.
- Chen JH, Lu JH, Pu XL, et al. Recyclable, malleable and intrinsically flame-retardant epoxy resin with catalytic transesterification. *Chemosphere*. 2022. <https://doi.org/10.1016/j.chemosphere.2022.133778>.
- Wang SH, Li JS, Wang WJ, et al. Silicone filled halloysite nanotubes for polypropylene composites: flame retardancy, smoke suppression and mechanical property. *Compos Part A Appl Sci Manuf*. 2021;140:106170. <https://doi.org/10.1016/j.compositesa.2020.106170>.
- Li X, Liu H, Jia X, et al. Novel approach for removing brominated flame retardant from aquatic environments using Cu/Fe-based metal-organic frameworks: a case of hexabromocyclododecane (HBCD). *Sci Total Environ*. 2018;621:1533–41. <https://doi.org/10.1016/j.scitotenv.2017.10.075>.
- Charitopoulou MA, Kalogiannis KG, Lappas AA, et al. Novel trends in the thermo-chemical recycling of plastics from WEEE containing brominated flame retardants. *Environ Sci Pollut Res*. 2020. <https://doi.org/10.1007/s11356-020-09932-5>.
- Cheng JJ, Niu SS, Zhao Y, et al. The flame retardant and thermal conductivity properties of high thermal conductivity expandable graphite microcapsule filled natural rubber composites. *Constr Build Mater*. 2022;318:125998. <https://doi.org/10.1016/j.conbuildmat.2021.125998>.
- Hanna AA, Abdelmoaty AS, Sherief MA. Synthesis, characterization, and thermal behavior of nanoparticles of Mg(OH)₂ to be used as flame retardants. *J Chem*. 2019. <https://doi.org/10.1155/2019/1805280>.
- Meng W, Wu W, Zhang W, et al. Bio-based Mg(OH)₂@M-Phyt: improving the flame-retardant and mechanical properties of flexible poly (vinyl chloride). *Polym Int*. 2019;68(10):1759–66. <https://doi.org/10.1002/pi.5885>.
- Ma J, Wang X, Li J, et al. Facile preparation of flame retardant cotton fabric via adhesion of Mg(OH)₂ by the assistance of ionic liquid. *Polymers*. 2020;12(2):259. <https://doi.org/10.3390/polym12020259>.
- Yao M, Wu H, Liu H, et al. In-situ growth of boron nitride for the effect of layer-by-layer assembly modified magnesium hydroxide on flame retardancy, smoke suppression, toxicity and char formation in EVA. *Polym Degrad Stab*. 2020;183:109417. <https://doi.org/10.1016/j.polyimdegradstab.2020.109417>.
- Sun H, Qi Y, Zhang J. Effect of magnesium hydroxide as a multifunctional additive on high solar reflectance, thermal emissivity, and flame retardancy properties of PP/SEBS/oil composites. *Polym Compos*. 2020;41(10):4010–9. <https://doi.org/10.1002/pc.25688>.
- Liu T, Wang F, Li G, et al. Magnesium hydroxide nanoparticles grafted by DOPO and its flame retardancy in ethylene-vinyl acetate copolymers. *J Appl Polym Sci*. 2021;138(1):49607. <https://doi.org/10.1002/app.49607>.
- Yang W, Wu S, Yang W, et al. Nanoparticles of polydopamine for improving mechanical and flame-retardant properties of an epoxy resin. *Compos B Eng*. 2020;186:107828. <https://doi.org/10.1016/j.compositesb.2020.107828>.
- Li Z, Liu L, González AJ, et al. Bioinspired polydopamine-induced assembly of ultrafine Fe(OH)₃ nanoparticles on halloysite toward highly efficient fire retardancy of epoxy resin via an action

- of interfacial catalysis. *Polym Chem.* 2017;8(26):3926–36. <https://doi.org/10.1039/C7PY00660H>.
21. Tawiah B, Yu B, Yuen ACY, et al. Facile preparation of uniform polydopamine particles and its application as an environmentally friendly flame retardant for biodegradable polylactic acid. *J Fire Sci.* 2020;38(6):485–503.
 22. Wang S, Du X, Deng S, et al. A polydopamine-bridged hierarchical design for fabricating flame-retarded, superhydrophobic, and durable cotton fabric. *Cellulose.* 2019;26(11):7009–23. <https://doi.org/10.1007/s10570-019-02586-8>.
 23. Ramezanpour M, Raeisi SN, Shahidi SA, et al. Polydopamine-functionalized magnetic iron oxide for the determination of trace levels of lead in bovine milk. *Anal Biochem.* 2019;570:5–12. <https://doi.org/10.1016/j.ab.2019.01.008>.
 24. Qiu S, Zhou Y, Ren X, et al. Construction of hierarchical functionalized black phosphorus with polydopamine: a novel strategy for enhancing flame retardancy and mechanical properties of polyvinyl alcohol. *Chem Eng J.* 2020;402:126212. <https://doi.org/10.1016/j.cej.2020.126212>.
 25. Lu YL, Ma J, Xu TY, et al. Preparation and properties of natural rubber reinforced with polydopamine-coating modified carbon nanotubes. *Express Polym Lett.* 2017;1(11):21–34. <https://doi.org/10.3144/expresspolymlett.2017.4>.
 26. Zhang TM, Zhang W, Xi H, et al. Polydopamine functionalized cellulose-MXene composite aerogel with superior adsorption of methylene blue. *Cellulose.* 2021;28(7):4281–93. <https://doi.org/10.1007/s10570-021-03737-6>.
 27. Li B. A study of the thermal decomposition and smoke suppression of poly (vinyl chloride) treated with metal oxides using a cone calorimeter at a high incident heat flux. *Polym Degrad Stab.* 2002;78(2):349–56. [https://doi.org/10.1016/S0141-3910\(02\)00185-4](https://doi.org/10.1016/S0141-3910(02)00185-4).
 28. Wang N, Teng H, Zhang X, et al. Synthesis of a carrageenan-iron complex and its effect on flame retardancy and smoke suppression for waterborne epoxy. *Polymers.* 2019;11(10):1677. <https://doi.org/10.3390/polym11101677>.
 29. Shi C, Qian X, Jing J. Phosphorylated cellulose/Fe³⁺ complex: a novel flame retardant for epoxy resins. *Polym Adv Technol.* 2021;32(1):183–9. <https://doi.org/10.1002/pat.5073>.
 30. Wang X, Yin Y, Li M, et al. Hexagonal boron Nitride@ZnFe₂O₄ hybrid nanosheet: an ecofriendly flame retardant for polyvinyl alcohol. *J Solid State Chem.* 2020;287:121366. <https://doi.org/10.1016/j.jssc.2020.121366>.
 31. Zhang M, Cheng Y, Li Z, et al. Biomass chitosan-induced Fe₃O₄ functionalized halloysite nanotube composites: preparation, characterization and flame-retardant performance. *NANO.* 2019;14(12):1950154. <https://doi.org/10.1142/S1793292019501546>.
 32. Wang L, Zhang M, Li B. Thermal analysis and flame-retarded mechanism of composites composed of ethylene vinyl acetate and layered double hydroxides containing transition metals (Mn Co, Cu, Zn). *Appl Sci.* 2016;6(5):131. <https://doi.org/10.3390/app6050131>.
 33. Younis AA, Faheim AA, Elsayy MM, et al. Novel flame retardant paint based on Co (II) and Ni (II) metal complexes as new additives for surface coating applications. *Appl Organomet Chem.* 2021;35(1):e6070. <https://doi.org/10.1002/aoc.6070>.
 34. Liu L, Pan Y, Zhao Y, et al. Self-assembly of phosphonate-metal complex for superhydrophobic and durable flame-retardant polyester-cotton fabrics. *Cellulose.* 2020;27(10):6011–25. <https://doi.org/10.1007/s10570-020-03148-z>.
 35. Jia MA, Du YH, Tay BY, et al. One-pot synthesis of Fe (III)-Polydopamine complex nanospheres: morphological evolution, mechanism and application of the carbonized hybrid nanospheres in catalysis and Zn-air battery. *Langmuir.* 2016;32:9265–75. <https://doi.org/10.1021/acs.langmuir.6b02331>.
 36. Zhang ZD, Qin JY, Yang RJ, et al. Synthesis of a novel dual layered double hydroxide hybrid nanomaterial and its application in epoxy nanocomposites. *Chem Eng J.* 2020. <https://doi.org/10.1016/j.cej.2019.122777>.
 37. Yun GW, Lee JH, Kim SH. Flame retardant and mechanical properties of expandable graphite/polyurethane foam composites containing iron phosphonate dopamine-coated cellulose. *Polym Compos.* 2020;41(7):2816–28. <https://doi.org/10.1002/pc.25578>.
 38. Zhang J, Li Z, Zhang L, et al. Bimetallic metal-organic framework and graphene oxide nano-hybrids induced carbonaceous reinforcement towards fire retardant epoxy: a novel alternative carbonization mechanism. *Carbon.* 2019. <https://doi.org/10.1016/j.carbon.2019.07.003>.
 39. Cheng JJ, Niu SS, et al. The thermal behavior and flame retardant performance of phase change material microcapsules with modified carbon nanotubes. *Energy.* 2022;240:122821. <https://doi.org/10.1016/j.energy.2021.122821>.
 40. Huo SQ, Sai T, Ran SY, et al. A hyperbranched P/N/B-containing oligomer as multifunctional flame retardant for epoxy resins. *Compos B Eng.* 2022;234:109701. <https://doi.org/10.1016/j.compositesb.2022.109701>.
 41. Ye GF, Huo SQ, Wang C, et al. A novel hyperbranched phosphorus-boron polymer for transparent, flame-retardant, smoke-suppressive, robust yet tough epoxy resins. *Compos B Eng.* 2021;227:109395. <https://doi.org/10.1016/j.compositesb.2021.109395>.
 42. Guo F, Zhang YZ, Cai L, et al. Functionalized graphene with Platelet-like magnesium hydroxide for enhancing fire safety, smoke suppression and toxicity reduction of Epoxy resin. *Appl Surf Sci.* 2022;578:152052. <https://doi.org/10.1016/j.apsusc.2021.152052>.
 43. Li Z, Liu ZQ, Wang DY, et al. Interfacial engineering of layered double hydroxide toward epoxy resin with improved fire safety and mechanical property. *Compos B Eng.* 2018;152:336–46. <https://doi.org/10.1016/j.compositesb.2018.08.094>.
 44. Qiu X, Kundu CK, Li Z, et al. Layer-by-layer-assembled flame-retardant coatings from polydopamine-induced in situ functionalized and reduced graphene oxide. *J Mater Sci.* 2019;54(21):13848–62. <https://doi.org/10.1007/s10075-019-03879-w>.
 45. Yue X, Li C, Ni Y, et al. Flame retardant nanocomposites based on 2D layered nanomaterials: a review. *J Mater Sci.* 2019;54(20):13070–105. <https://doi.org/10.1007/s10853-019-03841-w>.
 46. Li Z, Zhang JH, Wang DY, et al. Ultrafine nickel nanocatalyst-engineering of an organic layered double hydroxide towards a super-efficient fire-safe epoxy resin via interfacial catalysis. *J Mater Chem A.* 2018;6(18):8488–98. <https://doi.org/10.1039/C8TA00910D>.
 47. Wang Y, Li Z, Li Y, et al. Spray-drying-assisted layer-by-layer assembly of alginate, 3-aminopropyltriethoxysilane, and magnesium hydroxide flame retardant and its catalytic graphitization in ethylene-vinyl acetate resin. *ACS Appl Mater Interfaces.* 2018;10(12):10490–500. <https://doi.org/10.1021/acsami.8b01556>.
 48. Wang X, Hu W, Hu Y. Polydopamine-bridged synthesis of ternary h-BN@PDA@TiO₂ as nanoenhancers for thermal conductivity and flame retardant of polyvinyl alcohol. *Front Chem.* 2020;8:893. <https://doi.org/10.3389/fchem.2020.587474>.

Publisher's Note Springer Nature remains neutral with regard to jurisdictional claims in published maps and institutional affiliations.

Springer Nature or its licensor holds exclusive rights to this article under a publishing agreement with the author(s) or other rightsholder(s); author self-archiving of the accepted manuscript version of this article is solely governed by the terms of such publishing agreement and applicable law.